



Kosambi–Cartan–Chern Analysis of the Nonequilibrium Singular Point in One-Dimensional Elementary Catastrophe

Yamasaki, Kazuhito

Yajima, Takahiro

(Citation)

International Journal of Bifurcation and Chaos, 32(04):2250053

(Issue Date)

2022-03-30

(Resource Type)

journal article

(Version)

Accepted Manuscript

(Rights)

Electronic version of an article published as International Journal of Bifurcation and Chaos, vol. 32, no. 04, 2022, 2250053. DOI: 10.1142/S0218127422500535 © World Scientific Publishing Company. <http://www.worldscientific.com/worldscinet/ijbc>

(URL)

<https://hdl.handle.net/20.500.14094/90009140>



Kosambi-Cartan-Chern analysis of the non-equilibrium singular point in one-dimensional elementary catastrophe

Kazuhiro Yamasaki

*Department of Planetology, Graduate School of Science, Kobe University, Nada, Kobe 657-8501, Japan
yk2000@kobe-u.ac.jp*

Takahiro Yajima

*Department of Mechanical Systems Engineering, Faculty of Engineering, Utsunomiya University,
Utsunomiya, 321-8585, Japan
yajima@cc.utsunomiya-u.ac.jp*

Received (to be inserted by publisher)

1 This paper analyzes the properties of the non-equilibrium singular point in one-dimensional
2 elementary catastrophe. For this analysis, the Kosambi-Cartan-Chern (KCC) theory is applied
3 to characterize the dynamical system based on differential geometrical quantities. When both
4 the nonlinear connection and deviation curvature are zero, that is, when the geometric stability
5 of the KCC theory is neutral, two bifurcation curves are obtained: one is the known curve
6 with an equilibrium singular point, and the other is a new curve with a non-equilibrium singular
7 point. The two singular points are distinguished based on the vanishing condition of the Berwald
8 connection. Applied to the ecosystem described by the Hill function, the absolute value of the
9 cuspidal curvature of the non-equilibrium singular point is larger than that of the equilibrium
10 singular point. The ecological interpretation of this result is that the range of bistability of the
11 ecosystem in the non-equilibrium state is greater than that in the equilibrium state. The type
12 of singular points in equilibrium and non-equilibrium bifurcation curves are not necessarily the
13 same. For instance, there is a combination in which even if the former has one cusp, the latter
14 may show various types, depending on the parametric space. These results demonstrate that
15 there are cases where simply shifting the system from the equilibrium to non-equilibrium state
16 expands the range of bistability and changes the type of singularity. Although singularity analysis
17 is often performed near the equilibrium point, non-equilibrium analysis, i.e., analysis based on
18 the KCC theory, provides a useful perspective for analyzing singularity theory according to the
19 bifurcation phenomenon.

20 *Keywords:* singular point; KCC theory; bifurcation theory; non-equilibrium; elementary catastrophe; differential geometry

21 1. Introduction

22 The Kosambi-Cartan-Chern (KCC) theory can be used to characterize systems from the properties of
23 ordinary differential equations, such as bifurcation and stability, based on differential geometric quantities
24 (e.g., [Antonelli *et al.*, 1993; Yamasaki & Yajima, 2017; Gupta, & Yadav, 2019; Huang *et al.*, 2019; Chen *et al.*, 2020]). KCC theory has been well studied in the field of differential geometry, especially Finsler geometry
25 [Antonelli & Bucataru, 2001; Balan & Neagu, 2010; Neagu, 2013], and it has been applied to various fields
26

such as biology [Antonelli *et al.*, 2002] and physics [Boehmer & Harko, 2010; Harko & Sabău, 2008; Harko *et al.*, 2015; Dănilă *et al.*, 2016; Gupta & Yadav, 2017], among others [Liu *et al.*, 2021]. For instance, Yamasaki and Yajima (2020) performed KCC analysis of bifurcation phenomena including catastrophe. Given that catastrophe is closely related to the singularity of the system [Thom, 1972; Zeeman, 1977; Gilmore, 1981; Arnol'd, 2003; Izumiya *et al.*, 2016], this implies that the KCC and singularity theories are related through bifurcation phenomena. The main focus of catastrophe theory is, of course, the catastrophe shift exhibited by singularities, which are in a non-equilibrium state during the shift. Therefore, non-equilibrium stability analysis of the various shifts exhibited by singularities is necessary, but not sufficient. KCC theory has shown utility for non-equilibrium stability analysis. Thus, we performed KCC analysis of the basic singularities of catastrophe theory and analyzed their behavior in the non-equilibrium region.

The logistic equation with the Hill function is a typical example of a catastrophe in ecology [Ludwig *et al.*, 1978; Scheffer *et al.*, 2009; Strogatz, 2014]. Applying the KCC theory to this equation, we can derive the differential geometric quantities governing the stability of the system: nonlinear connection N_j^i and deviation curvature P_j^i . When both N_j^i and P_j^i are zero, i.e., the geometrical stability becomes neutral, we can obtain two bifurcation curves with a singular point [Yamasaki & Yajima, 2020]. (Their concrete forms are described by Eqs. (36) and (37) in Section 3.) The first is a known bifurcation curve with a singular point; however, the second curve with a singular point has not been fully analyzed. The main purpose of this study is to clarify the reason for the two types of singular points: the well-known equilibrium singular point and the lesser-known non-equilibrium singular point. Catastrophe theory is mainly concerned with singularities at equilibrium. However, as mentioned above, the catastrophe shift contains a non-equilibrium state. Here, we examine whether non-equilibrium singularities exist and their properties. The results are expected to provide a new perspective on singular points in relation to bifurcations. To quantitatively show the difference between equilibrium and non-equilibrium singularities, this study introduces the concept of curvature at a singularity. Calculations at singularities almost always fail; however, recent research has made it possible to calculate the curvature of singularities [Saji *et al.*, 2010; Umehara, 2011]. Comparing the curvature among singularities will reveal a case in which the range of bistable states increases by simply shifting the system from an equilibrium to non-equilibrium state.

From the viewpoint of catastrophe theory, there are various types of singular points [Thom, 1972; Arnol'd, 2003; Izumiya *et al.*, 2016]. In the case of the Hill function given above, we see that the singular points in the equilibrium and non-equilibrium states are of the same type, i.e., that of a cusp. However, this does not always hold. Here, we also consider the difference in the types of singular points between the two states based on well-known singular points in elementary catastrophe theory: cusp, swallowtail, and butterfly. This analysis will show, for instance, that there are combinations in which the equilibrium singular point is the cusp, but the non-equilibrium singular point is the swallowtail. This result indicates that the type of singularity changes when the system shifts from an equilibrium to non-equilibrium state, even if the control parameters do not change. Such non-equilibrium analysis will be possible by focusing on the basic geometric quantities in KCC theory, especially the deviation curvature and Berwald connection.

The structure of this paper is as follows. In Section 2, we provide a brief review of KCC theory in terms of time-like potential, and apply it to the normal form of elementary catastrophe as an example. In this example, there is one bifurcation curve with a singular point. In Section 3, we consider the logistic equation with the Hill function and show that there are two types of singular points: equilibrium and non-equilibrium ones. This result indicates the geometrical conditions necessary for the existence of non-equilibrium singularities. This condition is applied to the elementary catastrophe considered in Section 4, to show the existence and difference in non-equilibrium singular points among various parametric spaces. Section 5 provides our conclusions.

2. A brief review of KCC theory

2.1. *Differential geometrical quantities and stability*

The KCC theory was first applied to study the geometric invariance of second-order ordinary differential equations (ODEs) [Kosambi, 1933; Cartan, 1933; Chern, 1939; Antonelli *et al.*, 1993]. Since then, KCC theory has been applied to study the stability of dynamical systems (e.g., [Antonelli *et al.*, 1993; Udriste &

77 Nicola, 2009; Abolghasem, 2013; Yamasaki & Yajima, 2013]). Even more recently, numerous studies have
 78 investigated the geometric aspects of various dynamic structures, including those of physical (e.g., [Kumar *et*
 79 *al.*, 2019; Krylova *et al.*, 2019; Alawadi *et al.*, 2020; Liu *et al.*, 2020; Klën, & Molina, 2020; Wang *et al.*,
 80 2021]), biological (e.g., [Antonelli *et al.*, 2014; Antonelli *et al.*, 2019; Kolebaja, & Popoola, 2019; Mishra, &
 81 Tiwari, 2021]), and general (e.g., [Gupta, & Yadav, 2017; Sulimov *et al.*, 2018; Chen, & Yin, 2019; Feng *et*
 82 *al.*, 2020; Salnikova *et al.*, 2020; Liu *et al.*, 2021]) systems.

83 Let us consider the second-order ODE:

$$\ddot{x}^i + g^i(x, \dot{x}) = 0, \quad (1)$$

84 where $g^i(x, \dot{x})$ is a function. According to KCC theory, a small perturbation in the trajectory of (1) gives
 85 the covariant form of the variational equation (e.g., [Antonelli, & Bucataru, 2003]):

$$\frac{D^2 u^i}{Dt^2} = P_j^i u^j, \quad (2)$$

86 where $D(\dots)/Dt$ is a covariant differential, and the initial conditions are given by $u(0) = 0$ and $\dot{u}(0) \neq 0$.
 87 P_j^i is the geometric object or deviation curvature tensor, defined by the following relation:

$$P_j^i = -\frac{\partial g^i}{\partial x^j} + \frac{\partial N_j^i}{\partial x^k} \dot{x}^k - G_{jk}^i g^k + N_k^i N_j^k, \quad (3)$$

88 where N_j^i is a nonlinear connection:

$$N_j^i = \frac{1}{2} \frac{\partial g^i}{\partial \dot{x}^j}, \quad (4)$$

89 and G_{jk}^i is a Berwald connection:

$$G_{jk}^i = \frac{\partial N_j^i}{\partial \dot{x}^k}. \quad (5)$$

90 From the Berwald connection, the Douglas tensor is defined by $D_{jkl}^i = \partial G_{jk}^i / \partial \dot{x}^l$. Because this paper
 91 considers the one-dimensional case, we set $x^1 = x$, $g^1 = g$, $G_{11}^1 = G$, $N_1^1 = N$, $P_{11}^1 = P$, and $D_{11}^1 = D$ for
 92 simplicity.

93 The deviation curvature (3) determines the Jacobi stability of the system, i.e., the robustness of
 94 its trajectory [Sabău, 2005a; Harko *et al.*, 2016; Lake & Harko, 2016]. The trajectory of a one-dimensional
 95 system is Jacobi-stable when P is negative, and Jacobi-unstable when P is positive [Antonelli, & Bucataru,
 96 2003; Sabău, 2005a,b]. For convenience, we refer to the system as being J-stable when $P < 0$, as J-unstable
 97 when $P > 0$, and as J-neutral when $P = 0$. Moreover, we consider the nonlinear connection (4), as this
 98 is also related to the stability of the system ([Yamasaki & Yajima, 2013, 2016]). The system is considered
 99 to be N-stable when $N > 0$, as N-unstable when $N < 0$, and as N-neutral when $N = 0$. Around the
 100 equilibrium points, J-stable and J-unstable correspond to a spiral and a node, respectively [Sabău, 2005a].
 101 N-stable and N-unstable correspond to linear stable and linear unstable, respectively ([Yamasaki & Yajima,
 102 2013, 2016]). For instance, J-stable and N-stable around the equilibrium point correspond to a stable spiral
 103 (see [Yamasaki & Yajima, 2013] for more details).

104 2.2. Time-like potential and elementary catastrophe

105 The subject of KCC theory is a second-order ODE; thus, KCC theory cannot be applied to a first-order
 106 ODE. Antonelli *et al.*, (1993) introduced the production process concept, which enables the application
 107 of KCC theory to first-order ODEs such as the logistic equation. This second-order logistic equation has
 108 been applied to the real growth data of several species ([Antonelli, 1985; Antonelli *et al.*, 1993]), and to

109 evolution in biology ([Antonalli *et al.*, 2019, 2021]). The similar formulation has been also used to study
 110 transient behaviors during the production process, such as the effects of time feedback ([Hutchinson, 1948;
 111 Wright, 1955]). Moreover, Yamasaki and Yajima (2017) applied this technique to typical one-dimensional
 112 bifurcations described by first-order ODEs, such as saddle-node, transcritical, and pitchfork bifurcations,
 113 to obtain the same bifurcation as the original equation. Yamasaki and Yajima (2020) focused on the jump
 114 phenomenon (bifurcation), referred to as a catastrophic shift based on the time-like potential.

115 This paper defines x as a time-like potential of variable n . Time-like potentials do not always exist,
 116 because their existence essentially depends on properties of n such as integrability. In this paper, the
 117 variable n physically exists, whereas the time-like potential x is purely a mathematical construct. Therefore,
 118 it would be appropriate to express the analytical results in terms of n , rather than the time-like potential
 119 x . Specifically, this paper considers bifurcation stability, so it is appropriate to express the geometric
 120 quantities related to stability in terms of n . As we will see in the later section, the nonlinear connection
 121 related to N-stability and deviation curvature related to J-stability are expressed in terms of n in the last
 122 step. Thus, the time-like potential can be used as part of the analytical process, but is not necessary for
 123 the final interpretation of the bifurcation stability (see [Yamasaki & Yajima, 2020] for more details).

124 This paper applies the KCC theory to one-dimensional elementary catastrophe based on the time-like
 125 potential. We will show that the previous results can be obtained by an analysis based on the time-like
 126 potential. In addition, this approach allows for the analysis of non-equilibrium stability. Let us consider
 127 the dynamical system given by

$$\dot{n} = F(n), \quad (6)$$

128 where F is a function of n . This paper assumes that F and n satisfy the integrability conditions, so there
 129 is potential for f_c and x , as follows. In the elementary catastrophe, the potential function of the dynamical
 130 system, $f_c(n)$ is introduced as [Thom, 1972; Thompson, 1982]:

$$F = -\frac{\partial f_c}{\partial n} = -\partial_n f_c. \quad (7)$$

131 This paper uses the time-like potential defined by (e.g., [Antonelli *et al.*, 1993])

$$n = \frac{dx}{dt} = \dot{x}. \quad (8)$$

132 Therefore, this paper considers the equation:

$$\ddot{x} + \partial_n f_c(n) = 0. \quad (9)$$

133 That is, $g = \partial_n f_c(n)$ in the basic form of the KCC theory (1): $\ddot{x} + g = 0$. Therefore, the concrete forms
 134 of $f_c(n)$ give various differential geometrical quantities of the dynamical system. This paper considers the
 135 elementary catastrophe of one active variable given by the following, and the normal form [Thom, 1972;
 136 Poston, & Stewart, 1978]:

$$\text{Fold : } f_c(n) = \frac{n^3}{3} + an, \quad (10)$$

$$\text{Cusp : } f_c(n) = \frac{n^4}{4} + \frac{an^2}{2} + bn, \quad (11)$$

$$\text{Swallowtail : } f_c(n) = \frac{n^5}{5} + \frac{an^3}{3} + \frac{bn^2}{2} + cn, \quad (12)$$

$$\text{Butterfly : } f_c(n) = \frac{n^6}{6} + \frac{an^4}{4} + \frac{bn^3}{3} + \frac{cn^2}{2} + dn, \quad (13)$$

137 where a, b, c and d are parameters. Since the fold, i.e., saddle-node bifurcation, has already been considered
 138 [Yamasaki & Yajima, 2017], this paper will consider other types, specifically, the cusp, swallowtail, and
 139 butterfly. In the variable dynamical system with the time-like potential, the non-linear connection (4),
 140 Berwald connection (5), and deviation curvature (3) can be simplified as follows [Yamasaki & Yajima,
 141 2017]:

$$N = \frac{1}{2}\partial_{\dot{x}}g = \frac{1}{2}\partial_n g, \quad (14)$$

$$G = \partial_{\dot{x}}N = \partial_n N, \quad (15)$$

$$P = -Gg + N^2. \quad (16)$$

142 For elementary catastrophe, the equation of the bifurcation curve is derived from the condition: $\partial_n f_c =$
 143 0 and $\partial_n \partial_n f_c = 0$ [Thom, 1972]. From $g = \partial_n f_c$ and Eq. (14), this condition is expressed geometrically as

$$g = 0, N = 0. \quad (17)$$

144 In this section, the bifurcation curve is derived by this condition: N-stability is neutral ($N = 0$) in equilib-
 145 rium state ($g = 0$). The other quantities G and P are not relevant in this case. However, we derive them
 146 here as they are necessary for the non-equilibrium analysis discussed in the following section.

147 First, we consider the cusp defined by Eq. (11). From $g = \partial_n f_c$, Eqs. (14), (15), and (16) give the
 148 following geometric quantities:

$$N = \frac{1}{2}(3n^2 + a), \quad (18)$$

$$G = 3n, \quad (19)$$

$$P = \frac{1}{4}(-3n^4 - 6an^2 - 12bn + a^2). \quad (20)$$

149 Therefore, Eq. (17) gives the parametric equations of the bifurcation curve: $\gamma(n) = (b, a) = (2n^3, -3n^2)$.
 150 The curve has a cusp, as shown in the upper part of Fig. 1. The details of the figure are described in
 151 Section 2.3. Let us check the type of singular point with calculations. $d\gamma/dn|_{n=0} = \gamma'(0) = 0$ shows that
 152 the point $n = 0$ is the singular point. At the singular point, we obtain $\det(r'', r''') \neq 0$. This means that
 153 the type of singular point is cuspidal [Porteous, 2001; Izumiya *et al.*, 2016].

154 Next, we consider the swallowtail defined by Eq. (12). The same calculation used for the cusp case
 155 gives

$$N = 2n^3 + an + \frac{1}{2}b, \quad (21)$$

$$G = 6n^2 + a, \quad (22)$$

$$P = -ac - 3an^4 + \frac{b^2}{4} - 4bn^3 - 6cn^2 - 2n^6. \quad (23)$$

156 Equation (17) gives $b = -4n^3 - 2an$ and $c = 3n^4 + an^2$. Therefore, the bifurcation curve is a swallowtail
 157 type, as shown in the upper part of Fig. 2. Because the curve is recognized as the cross-section of the wave
 158 front $f(n, a) = (3n^4 + an^2, -4n^3 - 2an, a)$, we can obtain the identifier of the singularity from $\partial_n f \times \partial_a f$,
 159 as follows [Saji & Teramoto, 2020]: $\Lambda = 6n^2 + a$. At the singular point $n = 0$, we have $\partial_n \Lambda = 0$ and
 160 $\partial_n \partial_n \Lambda \neq 0$. This means that the type of singular point is swallowtail [Kokubo *et al.*, 2005; Fujimori *et al.*,
 161 2008; Saji *et al.*, 2009; Izumiya *et al.*, 2010].

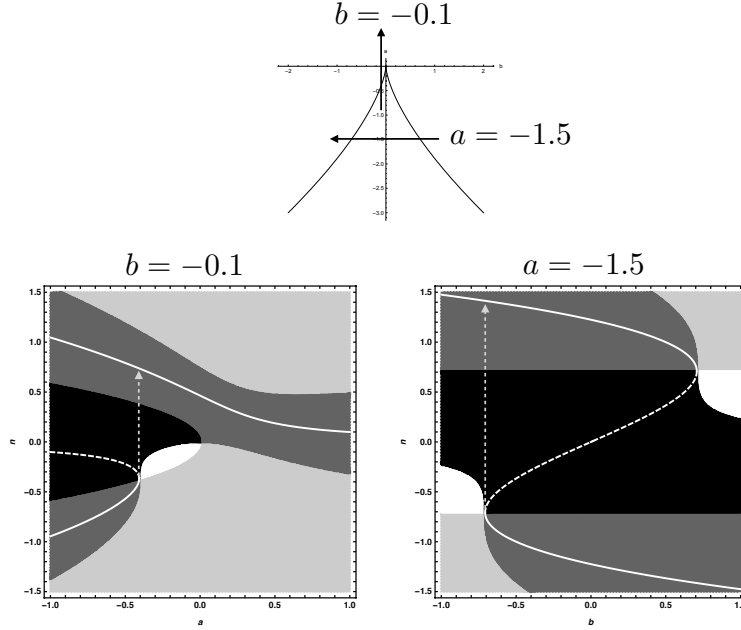


Fig. 1. Upper part shows the bifurcation curve with the cusp obtained by the condition $g = 0, N = 0$, i.e., the N-stability is neutral in the equilibrium state. By fixing the parameter, we obtain the lower part of the figure that shows the stable equilibrium curve (white solid line), the unstable equilibrium curve (white dotted line), and the KCC stability region described by the following gray-scale. The white region shows N-unstable and J-stable parts; the black region shows N-unstable and J-unstable parts; the light-gray region shows N-stable and J-stable parts; and the dark-gray region shows N-stable and J-unstable parts.

162 Finally, we consider the butterfly defined by Eq. (13). The same calculation used for the cusp case
 163 gives

$$N = \frac{1}{2} (3an^2 + 2bn + c + 5n^4), \quad (24)$$

$$G = 10n^3 + 3an + b, \quad (25)$$

$$P = \frac{1}{4} (3an^2 + 2bn + c + 5n^4)^2 - (3an + b + 10n^3) (an^3 + bn^2 + cn + d + n^5). \quad (26)$$

164 Equation (17) gives $c = -3an^2 - 2bn - 5n^4$ and $d = n^2(2an + b + 4n^3)$. Therefore, the bifurcation curve
 165 is of the butterfly type, as shown in the upper part of Fig. 3. The identifier of the singularity is given by
 166 $\Lambda = 10n^3 + b$ when $a \rightarrow 0, c \rightarrow -c$. This satisfies $\partial_n \Lambda(p) = \partial_n \partial_n \Lambda(p) = 0$ and $\partial_n \partial_n \partial_n \Lambda(p) \neq 0$ at the
 167 singular point p , so the singular point is a butterfly type [Izumiya, & Saji, 2010; Izumiya *et al.*, 2010].

168 As mentioned above, geometrical quantities related to stability, such as N , G , and P , are expressed
 169 in terms of n in the last step, so this paper uses the time-like potential as part of the analytical process.
 170 However, this does not mean that the time-like potential is always a purely mathematical concept, even in
 171 other analyses. Especially with unusual phenomena in which production processes (history) predominate,
 172 it becomes an explicit quantity. For instance, if we consider the number of paleontological species as n ,
 173 the number of fossils x observed in the stratum that formed during sedimentation is proportional to the
 174 time integral of n (e.g., [Raup & Stanley, 1978]). The differential form of this relationship corresponds to
 175 Eq. (8). Another example is the free rotation of a rigid body system, in which n corresponds to angular
 176 velocities and x corresponds to the Euler angles; here, the general form of Eq. (8) reveals the non-holonomic
 177 geometric structures of a rigid body system [Yajima *et al.*, 2018].

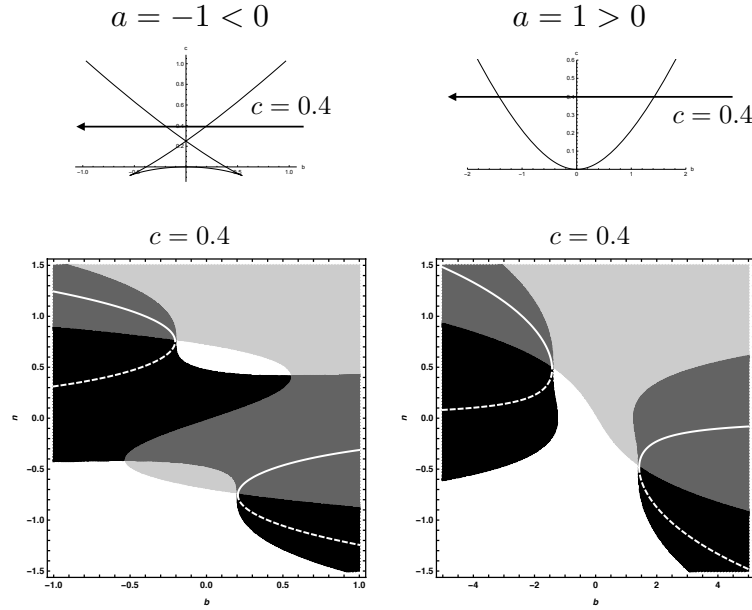


Fig. 2. Upper part shows the bifurcation curve with the swallowtail. The lower part is obtained by fixing the parameter and shows the KCC stability.

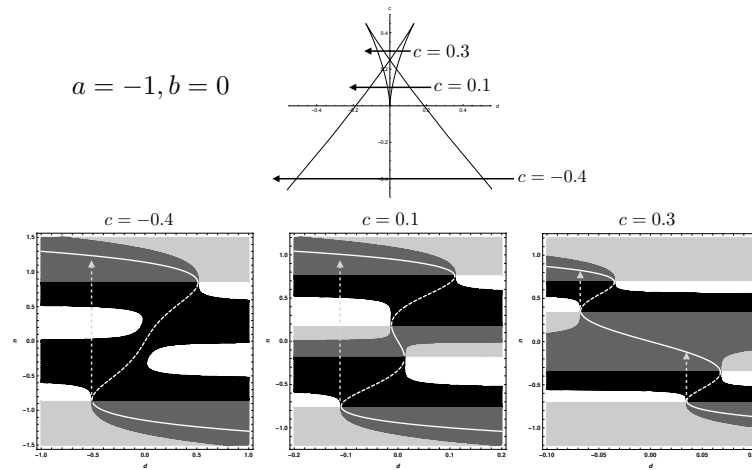


Fig. 3. Upper part shows the bifurcation curve with the butterfly. The lower part is obtained by fixing the parameter and shows the KCC stability.

178 **2.3. KCC stability of elementary catastrophe**

179 The upper parts of Figs. 1-3 show bifurcation curves with singularities in elementary catastrophe. The
 180 lower parts show the equilibrium curves (white solid and dotted lines) and the geometric stability in the
 181 non-equilibrium region (gray-scale region). The white solid line shows the stable equilibrium, and the white
 182 dotted line shows the unstable equilibrium. The white region shows N-unstable and J-stable parts; the black
 183 region shows N-unstable and J-unstable parts; the light gray region shows N-stable and J-stable parts; and
 184 the dark gray region shows N-stable and J-unstable parts. In the following paragraphs, we will look at the
 185 details of each figure. As the equilibrium results are similar, the difference in singularity can be seen by
 186 focusing on non-equilibrium stability, i.e., KCC analysis.

187 Figure 1 shows the bifurcation curve given by the set of coefficients (a, b) satisfying Eq. (17), which is
 188 confirmed to be cusp. The figure below shows the KCC stability of the cusp based on Eqs. (18) and (20).

189 Fixing $b = -0.1$ and crossing the cusp from bottom to top is the left side of the lower part of Fig. 1. This is
 190 a typical example of an incomplete bifurcation, i.e., the equilibrium curve (white curve) has separated into
 191 two parts. This separated region is the non-equilibrium region because it extends between the equilibrium
 192 curves. Equations (18) and (20) allow us to express the stability of this separated region (non-equilibrium
 193 region) as the gray scale. As the parameter a increases, a catastrophe occurs on the left side of the cusp
 194 (dotted arrow). Fixing $a = -1.5$ and crossing the cusp from right to left is the right side of the lower part
 195 of Fig. 1. Similarly, a catastrophe occurs on the left side of the cusp (dotted arrow). In both cases, the
 196 dotted arrow goes from the black region through the dark gray region. This is a typical result of stability
 197 change during the catastrophe process, as described in earlier works [Yamasaki & Yajima, 2020].

198 Figure 2 shows the bifurcation curve given by the set of coefficients (b, c) satisfying Eq. (17), which is
 199 confirmed to be swallowtail ($a < 0$) and fold ($a > 0$). The figure below shows the KCC stability based on
 200 Eqs. (21) and (23). Fixing $c = 0.4$ and crossing the bifurcation curves, the equilibrium curve (white curve)
 201 shows a similar separation pattern for $a < 0$ (Fig. 2 left) and $a > 0$ (Fig. 2 right), but the stability of the
 202 non-equilibrium region (gray scale) is different.

203 Figure 3 shows the bifurcation curve given by the set of coefficients (d, c) satisfying Eq. (17), which is
 204 confirmed to be butterfly. The figure below shows the KCC stability based on Eqs. (24) and (26). Since
 205 b is bias parameter [Bröcker, & Lander, 1975], we set $b = 0$ for simplicity in Fig. 3. Moreover, since case
 206 $a > 0$ is essentially the same as a cusp, we will only analyze case $a < 0$. The bending pattern of the
 207 equilibrium curve in the lower left of Fig. 3 ($c = -0.4$) is typical in catastrophe phenomena. For instance,
 208 the cusp in the lower right of Fig. 1 ($a = -1.5$) shows a similar bending pattern. However, the stability of
 209 the non-equilibrium region, i.e., during the catastrophe process (dotted arrow), can vary as follows. The
 210 arrow on the lower left of Fig. 3 ($c = -0.4$) passes through the white region. At the bottom center of Fig.
 211 3 ($c = 0.1$), the arrow passes through the light gray region (N-stable and J-stable). It is interesting that
 212 the most stable region exists in the non-equilibrium region. The bottom right of Fig. 3 ($c = 0.3$) shows a
 213 pattern unique to butterfly, where two catastrophic shifts occur. This is different from the others, but the
 214 non-equilibrium region is a typical pattern, i.e., transition from a black to dark-gray region.

215 2.4. Douglas tensor of elementary catastrophe

216 The analysis in the previous section shows that non-equilibrium stability during the catastrophic shift can
 217 vary, even though the pattern of the equilibrium curve is similar. Previous analyses have shown that the
 218 Douglas tensor is useful for describing stability changes during catastrophic shifts [Yamasaki & Yajima,
 219 2020]; thus, here we apply the method to elementary catastrophe. We can see that just as KCC stability is
 220 represented by the combination of the non-linear connection N and deviation curvature P , changes in KCC
 221 stability during the shift are represented by the combination of the Berwald connection G and Douglas
 222 tensor D .

223 The catastrophic shifts shown in Figs. 1-3 occur in the vertical (n -axis direction); thus, it is necessary
 224 to consider the change in stability along the n -axis. Then, we consider the expression of P (J-stability)
 225 differentiated into n [Yamasaki & Yajima, 2020]:

$$\frac{dP}{dn} = D \frac{dn}{dt}, \quad (27)$$

226 where D is the Douglas tensor [Douglas, 1927]. The Douglas tensor is one of the invariants of KCC theory
 227 (Douglas, 1927). In one-dimensional space, it is defined by $D = \partial_n G$; thus, combining Eqs. (1), (3), (4),
 228 and (5) gives Eq. (27). Because this contains dn/dt , it is essentially an equation for the non-equilibrium
 229 region. Geometrically, this equation shows that the Douglas tensor affects the deviation curvature during
 230 a catastrophic shift. In the one-dimensional case, $D = \partial_n G$, so calculating D for each catastrophe from
 231 (19), (22), and (25) gives

$$D_{\text{cusp}} = 3, \quad (28)$$

$$D_{\text{swallowtail}} = 12n, \quad (29)$$

$$D_{\text{butterfly}} = 30n^2 + 3a. \quad (30)$$

232 $D_{\text{butterfly}}$ contains the parameter a . When $a > 0$ i.e., $D > 0$, it is the same as the cusp. When $a < 0$,
 233 it can be factored as $D = 30(n + \sqrt{-a/10})(n - \sqrt{-a/10})$, such that $dP/dn < 0$ is valid. Therefore, even
 234 if $P > 0$ at the start of the shift (i.e., equilibrium point), there can be regions where $P < 0$ during the
 235 shift (i.e., non-equilibrium region/s). For instance, we see the shift of the lower left of Fig. 3, in which
 236 $c = -0.4$, $d \approx -0.51$, and $dn/dt > 0$ (arrow direction). The calculations show that the range $dP/dn < 0$ is
 237 $-0.32 < n < 0.32$ from $D \propto (n + 0.32)(n - 0.32)$, and the range $P < 0$ is $0.026 < n < 0.51$ from Eq. (26).

238 In a similar fashion, the Berwald connection $G = \partial N/\partial n$ controls N-stability during catastrophic shifts.
 239 In the case of butterfly without "bias" (i.e., $b = 0$), the Berwald connection is given by $G = 3an + 10n^3$. As
 240 shown in the center of Fig. 3, when $c = 0.1$ and there is a shift, $dn/dt > 0$; thus, from the calculations, the
 241 range $\partial N/\partial n > 0$ is $-0.55 < n < 0$ and $n > 0.55$ from $G \approx 10(n + 0.55)n(n - 0.55)$, and the range $N > 0$ is
 242 $-0.19 < n < 0.19$ and $n > 0.75$ from (24). An N-stable region exists in non-equilibrium, $-0.19 < n < 0.19$;
 243 thus, the light-gray region (N-stable and J-stable) can exist in the range $0.01 < n < 0.19$.

244 As can be seen from Eqs. (28) and (29), the Douglas tensor for cusp and swallowtail are either constant
 245 or linear in n , such that the stability pattern during a catastrophic shift is not as complicated as for the
 246 butterfly above.

247 3. Non-equilibrium singular point of the Hill function

248 3.1. Bifurcation curve and differential geometrical quantities

249 In ecology, the logistic equation with the Hill function is a typical example of a catastrophe [Ludwig *et*
 250 *al.*, 1978; Scheffer *et al.*, 2009; Strogatz, 2014]. KCC analysis, however, shows that its bifurcation curve
 251 has different characteristics from the elementary catastrophe considered in Section 2, as shown below. As
 252 mentioned in Section 2.2, this paper considers the following dynamical system:

$$\dot{n} + g = 0, \quad (31)$$

253 where $g = \partial_n f_c(n)$ with f_c as the potential function. The potential function of the logistic equation is
 254 $(n^3 r)/(3K) - (n^2 r)/2$, and that of the Hill function is $n - \tan^{-1}(n)$ from $n^2/(1 + n^2) = 1 - 1/(1 + n^2)$.
 255 Therefore, the potential function f_c of the logistic equation with the Hill function is given by

$$f_c = \frac{n^3 r}{3K} - \frac{n^2 r}{2} + n - \tan^{-1}(n).$$

256 In ecology, n , r , and K are all positive and correspond to biomass, the growth rate, and the carrying
 257 capacity, respectively. The potential f_c has the following known form:

$$g = \partial_n f_c = -rn + \frac{r}{K}n^2 + \frac{n^2}{1 + n^2}. \quad (32)$$

258 Therefore, Eqs. (14), (15), and (16) give the differential geometrical quantities of the system:

$$N = n \left(\frac{r}{K} + \frac{1}{(n^2 + 1)^2} \right) - \frac{r}{2}, \quad (33)$$

$$G = \frac{r}{K} + \frac{1 - 3n^2}{(n^2 + 1)^3}, \quad (34)$$

$$P = -\frac{n^3 r (4K + n^3 - 3n)}{K (n^2 + 1)^3} + \frac{3n^4}{(n^2 + 1)^4} + \frac{r^2}{4}. \quad (35)$$

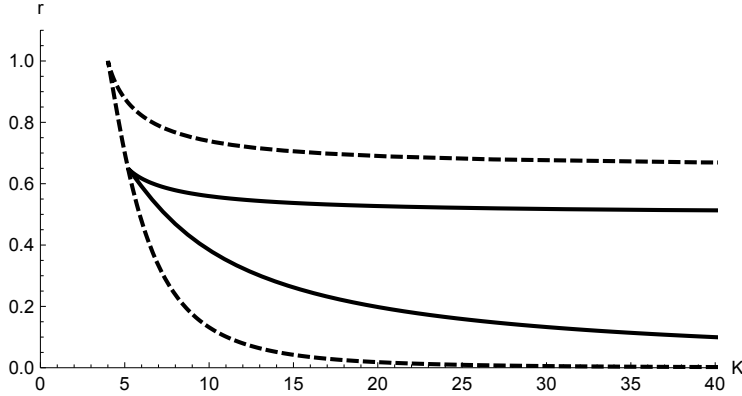


Fig. 4. Two bifurcation curves with cusps obtained by the condition: $N = 0, P = 0$, i.e., the stability is neutral. The solid line is the equilibrium curve ($G|_{N_0 P_0} \neq 0$) given by Eq. (36). The dotted line is the non-equilibrium curve ($G|_{N_0 P_0} = 0$) given by Eq. (37).

259 Yamasaki and Yajima (2020) showed that when $N = 0$ and $P = 0$, i.e., the geometrical stability
 260 is neutral, we can obtain the parametric equations of the bifurcation curve. Let K, r that satisfies the
 261 conditions of $N = 0$ and $P = 0$ be K_0, r_0 . In this case, Eqs. (33) and (35) give the following two bifurcation
 262 curves:

$$\gamma(K_0, r_0) = \left(\frac{2n^3}{n^2 - 1}, \frac{2n^3}{(n^2 + 1)^2} \right), \quad (36)$$

or

$$\gamma(K_0, r_0) = \left(\frac{8n^3}{3n^2 - 1}, \frac{8n^3}{(n^2 + 1)^3} \right). \quad (37)$$

263 Figure 4 shows the parametric plots of Eqs. (36) and (37). The cusp is observed in both cases. The solid line
 264 given by Eq. (36) agrees with the known bifurcation curve (e.g., [Strogatz, 2014]). The dotted line given
 265 by Eq. (37) is the new bifurcation curve obtained from KCC analysis. Yamasaki and Yajima (2020) did
 266 not provide a sufficient reason for the existence of this new solution (37); thus, we consider it here. Based
 267 on this consideration, the concept of bifurcation curves in non-equilibrium states will be presented. This
 268 bifurcation curve has a singular point, which implies the existence of a singular point in the non-equilibrium
 269 state.

270 **3.2. Non-equilibrium singular point**

271 As described in Section 2.2, the bifurcation curve of the dynamical system can be derived by (17): $g =$
 272 $0, N = 0$. From $\dot{n} + g = 0$, this gives $\dot{n} = 0$, i.e., an equilibrium state. Moreover, Eq. (16): $P = -Gg + N^2$
 273 shows $P = 0$. Therefore, the bifurcation curve in equilibrium satisfies the following equation:

$$N = 0, P = 0. \quad (38)$$

274 Conversely, let us consider the bifurcation curve starting from condition (38). From $P = -Gg + N^2$, this
 275 means $Gg = 0$. Let the parametric set that satisfies the condition (38) be $N_0 P_0$. For instance, the compo-
 276 nents (K_0, r_0) in Eqs. (36) and (37) correspond to this. The equation $Gg = 0$ means three combinations:

$$g|_{N_0 P_0} = 0, G|_{N_0 P_0} \neq 0, \quad (39)$$

$$g|_{N_0 P_0} \neq 0, G|_{N_0 P_0} = 0, \quad (40)$$

$$g|_{N_0P_0} = G|_{N_0P_0} = 0. \quad (41)$$

277 The relation (39) gives a known equilibrium bifurcation curve, as described earlier. In this case, the Berwald
 278 connection G is generally non-zero. When G vanishes, the relation (40) holds and gives another bifurcation
 279 curve. Since $g \neq 0$ means $\dot{n} \neq 0$, this is in the non-equilibrium state. The relation (41) does not hold in gen-
 280 eral, but is valid at the equilibrium singular point. Equations (40) and (42) describe the geometric relation
 281 for the usual singularity in the equilibrium state, while Eq. (41) pertains to the non-equilibrium states.
 282 We cannot discuss non-equilibrium singularities without considering the Berwald connection introduced
 283 by KCC theory.

284 Let us check the above results using the Hill function. The substitution of the parametric set satisfies
 285 (38), i.e., the components of (36) into (32) and (34) gives the relation (39):

$$g|_{K_0,r_0} = 0, \quad G|_{K_0,r_0} = \frac{n^2(n^2 - 3)}{(n^2 + 1)^3}. \quad (42)$$

286 Since $\dot{n} = 0$ from $\dot{n} + g = 0$, it is confirmed that the known solution (36) is the bifurcation curve in
 287 equilibrium. The substitution of the components of (37) into (32) and (34) gives the relation (40):

$$g|_{K_0,r_0} = \frac{n^4(n^2 - 3)}{(n^2 + 1)^3}, \quad G|_{K_0,r_0} = 0. \quad (43)$$

288 Since $\dot{n} \neq 0$ in general, the new solution (37) is the bifurcation curve in non-equilibrium. Thus, the condition
 289 $N = 0, P = 0$ in the KCC theory encompasses not only the known equilibrium bifurcation curve (36), but
 290 also the non-equilibrium bifurcation curve (37). As can be seen from Fig. 4, the bifurcation curve (36) and
 291 (37) are tangent at the equilibrium singular point $n = \sqrt{3}$. At the point, $G|_{K_0,r_0}$ in (42) and $g|_{K_0,r_0}$ in (43)
 292 become zero, such that the relation (41) holds.

293 Let us consider the condition under which two bifurcation curves can be obtained, such as (36) and
 294 (37). Two equations for the bifurcation curve require a quadratic equation for the coefficients. Since the
 295 nonlinear connection is linear with respect to g from $N = (1/2)\partial_n g$, the equation $N = 0$ does not correspond
 296 to this. On the other hand, from $P = -Gg + N^2$, the deviation curvature contains a nonlinear term, so
 297 the equation $P = 0$ is needed for two bifurcation curves. Moreover, the coefficients of the variables are
 298 important because they remain after differentiation by n . In other words, when considering the coefficients
 299 of the constant term, only one bifurcation curve is obtained (examples will be given in Section 4). In the
 300 case of the Hill function, the relation (40) can be obtained because Eq. (32) shows that all of the coefficients
 301 K, r are on the variable n . Usually, if there is a single bifurcation curve, it is an equilibrium one.

3.3. Cuspidal curvature of a non-equilibrium singular point

302 In Fig. 4, both equilibrium and non-equilibrium singular points appear to be cusps. This can be confirmed
 303 using the discriminant condition [Porteous, 2001]. The results of this calculation can be used to estimate
 304 curvature at the singular point [Umehara, 2011; Saji *et al.*, 2010; Shiba & Umehara, 2012]. This is useful
 305 for quantifying the differences between equilibrium and non-equilibrium cusps.

306 First, we consider the equilibrium bifurcation curve (36). The derivative gives
 307

$$\frac{d\gamma}{dn} = \gamma' = \left\{ \frac{2n^2(n^2 - 3)}{(n^2 - 1)^2}, -\frac{2n^2(n^2 - 3)}{(n^2 + 1)^3} \right\}. \quad (44)$$

308 This is zero at $n = \sqrt{3}$ in $n > 0$, so it is the singular point. Moreover, $\det(\gamma'', \gamma''')$ gives

$$\left| \begin{array}{cc} \frac{4n(n^2+3)}{(n^2-1)^3} & \frac{4n(n^4-8n^2+3)}{(n^2+1)^4} \\ -\frac{12(n^4+6n^2+1)}{(n^2-1)^4} & -\frac{12(n^6-15n^4+15n^2-1)}{(n^2+1)^5} \end{array} \right| = \frac{192n^3(3n^6 - 7n^4 - 27n^2 + 15)}{(n^2 - 1)^4(n^2 + 1)^5}. \quad (45)$$

This is not zero at $n = \sqrt{3}$. Since $\gamma' = 0$ and $\det(\gamma'', \gamma''') \neq 0$ at the singular point, the discriminant condition shows that the type of equilibrium singular point is cusp [Porteous, 2001; Izumiya *et al.*, 2016].

In a similar fashion, the non-equilibrium bifurcation curve (37) gives γ' and $\det(\gamma'', \gamma''')$ as follows:

$$\left\{ \frac{24n^2(n^2-1)}{(1-3n^2)^2}, -\frac{24n^2(n^2-1)}{(n^2+1)^4} \right\}, \quad (46)$$

$$\left| \frac{\frac{48(n^3+n)}{(3n^2-1)^3}}{48(9n^4+18n^2+1)} - \frac{\frac{48(2n^5-5n^3+n)}{(n^2+1)^5}}{48(10n^6-45n^4+24n^2-1)} \right| = -\frac{9216n^3(3n^6-34n^4+49n^2-10)}{(1-3n^2)^4(n^2+1)^5}. \quad (47)$$

At the singular point $n = 1$ ($\gamma' = 0$), we have $\det(\gamma'', \gamma''') \neq 0$. Therefore, the non-equilibrium singular point is also a cusp.

From the above calculations, it is confirmed using the Hill function that both the equilibrium and non-equilibrium singular points are cusp type. Of course, this has only been confirmed with the Hill function; in general, it is possible to have different types of singular points (e.g., swallowtail or butterfly). In fact, examples of this are provided in the next section.

Catastrophe theory, which was introduced in the 1960s, has influenced various research areas (e.g., singularity theory). Recently, Umehara (2011) introduced the new concept of singular curvature at the cusp. Saji *et al.* (2010) considered cuspidal curvature based on the duality between singular points and inflection points. According to recent studies, we can characterize the system in terms of curvature even at the singular point [Umehara, 2011; Saji *et al.*, 2010; Shiba & Umehara, 2012]. Thus, we estimate the curvature of the two singular points in Fig. 4 and show that they are the same in terms of quality (both cusp) but differ in quantity. When the curve $\gamma(n)$ has a cusp at $n = c$, the cuspidal curvature is defined as [Saji *et al.*, 2010; Shiba & Umehara, 2012]:

$$\mu = \frac{\det(\gamma''(c), \gamma'''(c))}{|\gamma''(c)|^{5/2}}. \quad (48)$$

Since $\det(\gamma'', \gamma''') \neq 0$ at the cusp, the cuspidal curvature is always non-zero. If the sign of the curvature is positive (negative), it is called zig (zag), and the bifurcation curve turns to the right (left) of the growth direction at the singular point (Fig. 4.1 in [Saji *et al.*, 2010]). The sign is invariant under an orientation preserving diffeomorphism of the plane [Shiba & Umehara, 2012]. That is, the sign changes when the orientation of the curve is reversed. The magnitude of the curvature indicates the degree of opening of the cusp. The number $(1/\mu)^2$ is called the cuspidal curvature radius, which corresponds to the radius of the best approximating cycloid at the cusps ([Saji *et al.*, 2010; Shiba & Umehara, 2012]).

Using the results of Eqs. (45) and (47), Eq. (48) indicates that the cuspidal curvature of the equilibrium singular point is about -0.047 and that of the non-equilibrium singular point is about -0.27 . The difference in magnitude of cuspidal curvature reflects the difference in the degree of the opening of the two bifurcation curves, as shown in Fig. 4. This enclosed area is the so-called bistable state, where rapid changes in biomass occur [Ludwig *et al.*, 1978; Scheffer *et al.*, 2009; Strogatz, 2014]. Thus, this phenomenon occurs over a wider range of parameters in the non-equilibrium regime. In this way, calculation of the cuspidal curvature at the singular point is useful for identifying the range of bistable states in parametric space.

As mentioned above, studies of singular curvature are mainly mathematical. Therefore, it is useful to show that singular curvature is also applicable to natural science and gives an important perspective. For instance, the range of bistable states of the ecosystem, and usually changes with the form of the equation. However, the results of this paper show that the cusp curvature of the non-equilibrium state is larger than that of the equilibrium state. Thus, the range of bistable states is increased simply by shifting the system from an equilibrium state to a non-equilibrium state, even if the equation itself does not change. It has long been accepted that actual ecosystems may be in a state of non-equilibrium [Pickett, 1980; Sprugel, 1991; Mori, 2011]; thus, singularity curvature is useful for interpreting the diversity of ecosystems.

348 In the above, only cuspidal curvature is considered; however, there are various geometric invariants
 349 that characterize a singular point, such as cusp-directional torsion, singular curvature, and so on[Saji *et*
 350 *al.*, 2009; Hasegawa *et al.*, 2015; Martins, & Saji, 2016; Martins *et al.*, 2016]. Based on these geometric
 351 quantities, a more detailed analysis of the singular point of the ecosystem is a future research target.

352 4. Non-equilibrium singular point of elementary catastrophe

353 In Section 2, we analyzed the singular points of elementary catastrophe from the geometrical expression
 354 of known viewpoints as (17): $g = 0, N = 0$, i.e., the N-stability is neutral in equilibrium. In this section,
 355 we reanalyze it from the viewpoint obtained in Section 3 as (38): $N = 0, P = 0$, i.e., stability is neutral.
 356 The latter viewpoint does not include g ; thus, it does not matter whether it is in equilibrium or not.
 357 Since the bifurcation curve is related to linear stability, the neutral condition for N-stability ($N = 0$) is
 358 necessary for both viewpoints. Moreover, one more equation is needed to obtain two variables describing
 359 the bifurcation curve. The previous analysis used the equilibrium state ($g = 0$), whereas here we use the
 360 J-stability ($P = 0$). Since the deviation curvature P is introduced by KCC theory, the theory is useful for
 361 considering the non-equilibrium singular point.

362 4.1. Cusp

363 We will show that the normal form of a cusp contains only an equilibrium singular point. The dynamical
 364 system with a cusp is $\dot{n} + g = 0$ with

$$g = n^3 + an + b. \quad (49)$$

365 Thus, as obtained in Section 2.2, the differential geometric quantities of cusp can be obtained from equations
 366 (14), (15), and (16). For convenience, we redescribe the results:

$$N = \frac{1}{2}(3n^2 + a), \quad G = 3n, \quad P = \frac{1}{4}(-3n^4 - 6an^2 - 12bn + a^2). \quad (50)$$

367 Therefore, the solutions (a_0, b_0) of (38): $N = 0, P = 0$, give the following bifurcation curve:

$$\gamma(a_0, b_0) = (-3n^2, 2n^3). \quad (51)$$

368 This is the known equilibrium bifurcation curve of cusp (Fig. 1). In fact, from (51), $g|_{a_0, b_0} = 0$ and $G = 3n$
 369 is generally non-zero, so the relation (39) is satisfied.

370 4.2. Swallowtail

371 The dynamical system with swallowtail is $\dot{n} + g = 0$ with

$$g = n^4 + an^2 + bn + c. \quad (52)$$

372 We redescribe the differential geometric quantities of swallowtail obtained in Section 2.2:

$$N = 2n^3 + an + \frac{1}{2}b, \quad G = 6n^2 + a, \quad P = -ac - 3an^4 + \frac{b^2}{4} - 4bn^3 - 6cn^2 - 2n^6. \quad (53)$$

373 Therefore, from the solutions (b_0, c_0) of (38),

$$\gamma(b_0, c_0) = (-2(an + 2n^3), n^2(a + 3n^2)). \quad (54)$$

374 This gives the known equilibrium bifurcation curve of swallowtail (Fig. 2). From $g|_{b_0, c_0} = 0, G|_{b_0, c_0} = 6n^2 + a$,
 375 the relation (39) is satisfied. In the (b, c) -space of swallowtail, the identifier of singularity Λ is equal to

the Berwald connection G , so the vanishing condition $\Lambda = 0$ at the equilibrium singular point corresponds to the relation (41). In this case, the condition of discrimination (differentiation of Λ) is related to the Douglas tensor.

Next, we consider the solutions (a_0, c_0) of (38):

$$\gamma(a_0, c_0) = \left(\frac{-b - 4n^3}{2n}, \frac{1}{2} (2n^4 - bn) \right). \quad (55)$$

Since $g|_{a_0, c_0} = 0$, $G|_{a_0, c_0} = 4n^2 - b/2n$, this also gives the equilibrium bifurcation curve.

Finally, we consider that the combination does not contain a coefficient of the constant term: c , that is, (a, b) . In this case, we can obtain two solutions of Eq. (38):

$$\gamma(a_0, b_0) = (-6n^2, 8n^3), \quad (56)$$

$$\gamma(a_0, b_0) = \left(\frac{c - 3n^4}{n^2}, \frac{2(n^4 - c)}{n} \right). \quad (57)$$

The curve (56) gives $g|_{a_0, b_0} = c + 3n^4$, $G|_{a_0, b_0} = 0$, i.e., the relation (40), so it is a non-equilibrium one. Therefore, the point $n = 0$ is a non-equilibrium cusp. The curve (57) gives $g|_{a_0, b_0} = 0$, $G|_{a_0, b_0} = (c + 3n^4)/n^2$, i.e., the relation (39); thus, it is an equilibrium one.

4.3. *Butterfly*

The dynamical system with butterfly is $\dot{n} + g = 0$ with

$$g = n^5 + an^3 + bn^2 + cn + d. \quad (58)$$

We redescribe the differential geometric quantities of butterfly obtained in Section 2.2:

$$N = \frac{1}{2} (3an^2 + 2bn + c + 5n^4), \quad (59)$$

$$G = 10n^3 + 3an + b, \quad (60)$$

$$P = \frac{1}{4} (3an^2 + 2bn + c + 5n^4)^2 - (3an + b + 10n^3) (an^3 + bn^2 + cn + d + n^5). \quad (61)$$

Therefore, the solutions (c_0, d_0) of (38) give

$$\gamma(c_0, d_0) = (-3an^2 - 2bn - 5n^4, n^2 (2an + b + 4n^3)). \quad (62)$$

This gives the known equilibrium bifurcation curve for a butterfly type (Fig. 3). In fact, this gives $g|_{c_0, d_0} = 0$, $G|_{c_0, d_0} = 10n^3 + 3an + b$. As in the swallowtail case, the identifier of singularity in (c, d) -space is equal to the Berwald connection.

In the following, we consider combinations that do not contain a coefficient of the constant term: d . The solutions (a_0, b_0) of (38) give the equilibrium curve ($g|_{a_0, b_0} = 0$, $G|_{a_0, b_0} = (3d + cn + 3n^5)/n^2$):

$$\gamma(a_0, b_0) = \left(\frac{cn + 2d - 3n^5}{n^3}, \frac{-2cn - 3d + 2n^5}{n^2} \right), \quad (63)$$

and the non-equilibrium curve ($g|_{a_0, b_0} = (3d + cn + 3n^5)/3$, $G|_{a_0, b_0} = 0$):

$$\gamma(a_0, b_0) = \left(\frac{c - 15n^4}{3n^2}, \frac{5n^4 - c}{n} \right). \quad (64)$$

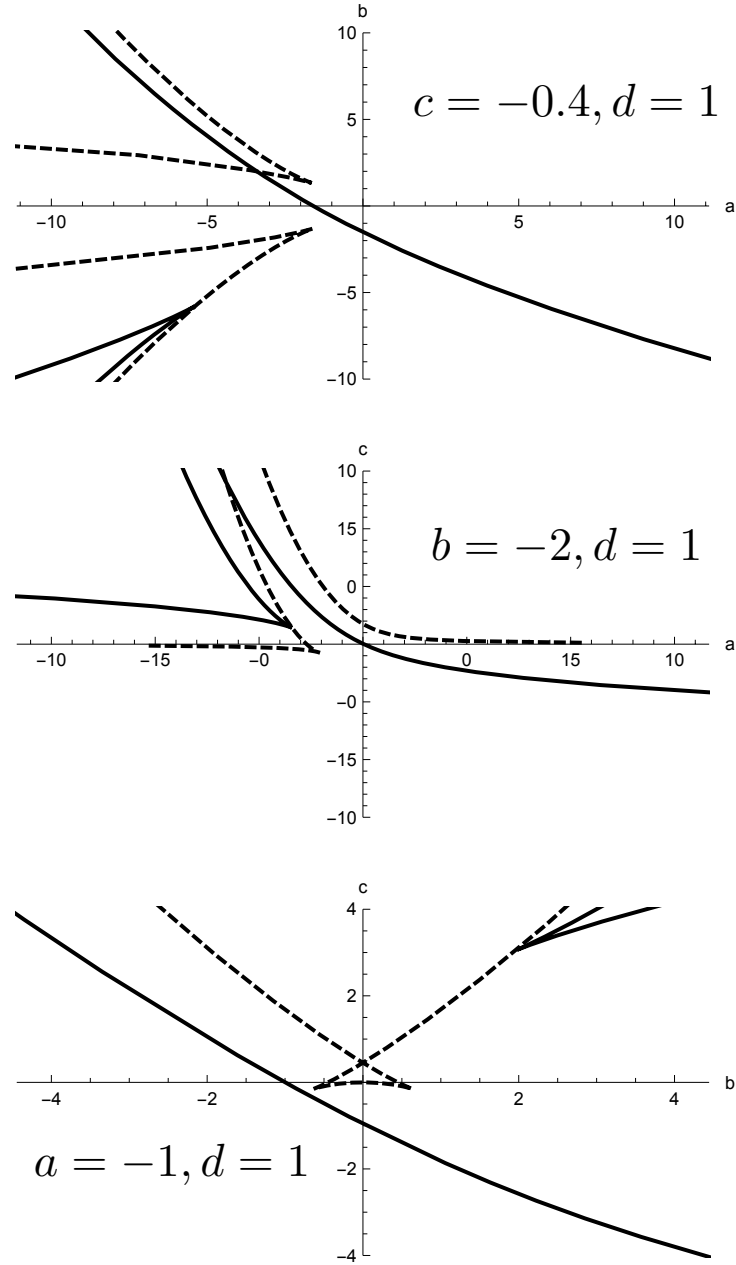


Fig. 5. Bifurcation curves for the combination of parameters do not contain a coefficient for the constant term d . The upper part is the parametric space (a_0, b_0) , the middle part is (a_0, c_0) , and the lower part is (b_0, c_0) . In each space, the solid line is the equilibrium bifurcation curve, and the dotted line is the non-equilibrium one.

396 For instance, if we consider the case of $c = -0.4, d = 1$ (upper of Fig. 5), the equilibrium curve (solid line)
 397 gives one cusp, whereas the non-equilibrium curve (dotted line) gives two cusps. The solutions (a_0, c_0) of
 398 (38) give the equilibrium curve $(g|_{a_0, c_0} = 0, G|_{a_0, c_0} = -b/2 + 3d/2n^2 + 4n^3)$:

$$\gamma(a_0, c_0) = \left(\frac{-bn^2 + d - 4n^5}{2n^3}, \frac{-bn^2 - 3d + 2n^5}{2n} \right), \quad (65)$$

and the non-equilibrium curve $(g|_{a_0, c_0} = (2/3)n^2(-b/2 + 3d/2n^2 + 4n^3), G|_{a_0, c_0} = 0)$:

$$\gamma(a_0, c_0) = \left(\frac{-b - 10n^3}{3n}, 5n^4 - bn \right). \quad (66)$$

399 For instance, if we consider the case of $b = -2, d = 1$ (middle of Fig. 5), both curves (solid line and
400 dotted line) have one cusp. The solutions (b_0, c_0) of (38) give the equilibrium curve ($g|_{b_0, c_0} = 0, G|_{b_0, c_0} =$
401 $d/n^2 + an + 6n^3$):

$$\gamma(b_0, c_0) = \left(\frac{-2an^3 + d - 4n^5}{n^2}, \frac{an^3 - 2d + 3n^5}{n} \right), \quad (67)$$

402 and the non-equilibrium curve ($g|_{b_0, c_0} = n^2(d/n^2 + an + 6n^3), G|_{b_0, c_0} = 0$):

$$\gamma(b_0, c_0) = (-3an - 10n^3, 3(an^2 + 5n^4)). \quad (68)$$

403 For instance, if we consider the case of $a = -1, d = 1$ (lower part of Fig. 5), the equilibrium curve (solid
404 line) gives one cusp and the non-equilibrium curve (dotted line) gives swallowtail.

405 The above results show that although the equilibrium bifurcation curve has one cusp regardless of
406 the parameters, the non-equilibrium bifurcation curve shows singular points that vary depending on the
407 parameters. This implies that the non-equilibrium singular points clarify the properties of catastrophe in
408 each parametric space. Moreover, bifurcation curves with non-equilibrium singular points are expected to
409 produce a diverse range of dynamical phenomena in nature. Usually, qualitative changes in the singularity
410 are accompanied by changes in the parameters. The lower part of Fig. 5 shows that there are cases where
411 the type of singularity changes from cusp to swallowtail, simply by changing from equilibrium to non-
412 equilibrium, even if the parameters do not change. Although singularity analysis is often performed near
413 the equilibrium point, this result indicates that non-equilibrium analysis, i.e. KCC theory, provides a useful
414 perspective for analyzing singularity theory.

415 5. Conclusions

416 Our main conclusions are as follows.

- 417 (1) KCC theory is applied to three kinds of singularities in elementary catastrophe theory; these singulari-
418 ties show various stabilities in the non-equilibrium region (Sections 2.2 and 2.3; Figs. 1 – 3). Although
419 the equilibrium curves of the cusp and butterfly show the same bending type, the change in stabil-
420 ity during the shift (i.e., the non-equilibrium state) is different (Section 2.4. Table 1). Therefore, the
421 differences in singularities become clearer when the analysis focuses on non-equilibrium stability, i.e.,
422 KCC analysis. Additionally, not only the stabilities, but also their changes during the shift, can be
423 described by the basic geometric quantities in KCC theory (Table 2).
- 424 (2) We have shown that the typical bifurcation curve can be derived from the neutrality of N-stability
425 in equilibrium (Section 2.2). We have also derived new types of bifurcation curves by considering the
426 neutrality of both J-stability and N-stability (Sections 3.1 and 3.2). Because P contains a nonlinear
427 term, its neutral condition is quadratic, so two bifurcation curves can be derived. In this case, a non-
428 equilibrium bifurcation curve is derived from the vanishing condition of the Berwald connection (Table
429 3). This curve contains a singularity, suggesting the existence of a non-equilibrium singularity. Given
430 that J-stability is unique to KCC theory, this result implies that KCC theory is useful for extending
431 the singularity theory to non-equilibrium fields. Just as singularities are closely related to ordinary
432 bifurcations, non-equilibrium singularities are closely related to non-equilibrium bifurcations.
- 433 (3) In the case of Hill functions, the cuspidal curvature of a non-equilibrium singular point is larger than
434 that of an equilibrium singular point (Section 3.3). Biologically, this is interpreted as follows: the range
435 of bistability of the ecosystem in the non-equilibrium state is greater than that in the equilibrium
436 state. This means that the range of bistable states increases as the system shifts from equilibrium to
437 non-equilibrium, even if the equation itself does not change (Fig. 4). Since the ecosystem is sometimes
438 in non-equilibrium, calculation of the curvature of each singularity (equilibrium and non-equilibrium)
439 is useful for understanding the diversity in nature.
- 440 (4) The singular points in equilibrium and non-equilibrium bifurcation curves are not necessarily the same
441 (Section 4, Fig. 5). For instance, in the case of a butterfly type, the former is always a cusp, whereas the

442
443
444
445

latter varies depending on the parametric space. This means that even if the parameters do not change, there are cases where the type of singularity changes when the system shifts from an equilibrium to non-equilibrium state (Table 4). Therefore, the existence of non-equilibrium singular points may produce a diverse range of dynamics.

Table 1. Stabilities of singular points. Abbreviations are defined as follows. WH: N-unstable & J-stable parts; BL: N-unstable & J-unstable parts; LG : N-stable & J-stable parts; and DG: N-stable & J-unstable parts.

	Equilibrium stability	Non-equilibrium stability during the shift
Cusp	Bending type	From BL to DG
Butterfly	Bending type	From BL to DG via WH and LG

Table 2. Stabilities and geometric quantities in KCC theory.

	Stability	Stability change during the shift
N-stability	Non-linear connection N	Berwald connection B
J-stability	Deviation curvature P	Douglas tensor D

Table 3. Types of bifurcation curves and their conditions in KCC theory.

	Equilibrium curve	Non-equilibrium curve
$g = 0, N = 0$	Always	NA
$N = 0, P = 0$	$G_{N_0 P_0} \neq 0$	$G_{N_0 P_0} = 0$

Table 4. Singular points in equilibrium and non-equilibrium curves considered in this paper.

	Equilibrium singular points	Non-equilibrium singular points
Cusp	Cusp	NA
Swallowtail	Swallowtail, Cusp	Cusp
Butterfly	Butterfly, Cusp	Swallowtail, Cusp

References

- 446
447 Abolghasem, H. [2013b] “Jacobi stability of hamiltonian systems,” *Int. J. Pure Appl. Math.* **87**, 181–194.
448 Antonelli, P., Rutz, S., & Strychar, K. B. “Heat stress on scleractinian corals: Its symbionts in evolution,”
449 *Nonlinear Anal. RWA.* **28**, 189–196.
450 Antonelli, P.L. [1985] *Mathematical Essays on Growth and the Emergence of Form*, (University of Alberta
451 Press, Alberta).
452 Antonelli, P.L., Ingarden, R.S. & Matsumoto, M. [1993] *The Theory of Sprays and Finsler Spaces with*
453 *Applications in Physics and Biology*, (Kluwer, Dordrecht).
454 Antonelli, P. L., & Bucataru, I. [2001] “New results about the geometric invariants in KCC-theory,” *An.*
455 *St. Univ. ”Al. I. Cuza” Iasi* **47**, 405–420.
456 Antonelli, P.L. & Bucataru, I. [2003] *KCC Theory of a System of Second Order Differential Equations,*
457 *in: Handbook of Finsler Geometry*, (Kluwer, Dordrecht).

- 458 Antonelli, P.L., Leandro, E.S. & Rutz, S.F. [2014] “Gradient-driven dynamics on Finsler manifolds: the
459 Jacobi action-metric theorem and an application in ecology,” *Nonlinear Stud.* **21**, 141–152.
- 460 Antonelli, P. L., Rutz, S. F. & Ferreira Jr, G.S. [2019] “Remarks on modeling serial endosymbiosis and
461 evolution of eukaryote tissue formation,” *Nonlinear Stud.* **26**, 653–662.
- 462 Antonelli, P.L., Rutz, S.F., & Sabău, S.V. [2002] “A transient-state analysis of Tyson’s model for the cell
463 division cycle by means of KCC-theory,” *Open Syst. Inf. Dyn.* **9**, 222–238.
- 464 Alawadi, M. A., Batic, D. & Nowakowski, M. [2020] “Light bending in a two black hole metric,” *Class.*
465 *Quantum Grav.* **38**, 045003.
- 466 Arnol’d, V. I. [2003] *Catastrophe Theory* (3rd), (Springer Science & Business Media).
- 467 Balan, V. & Neagu, M. [2010] “Jet geometrical extension of the KCC-invariants,” *Balkan J. Geom. Appl.*
468 **15**, 8–16.
- 469 Boehmer, C.G. & Harko, T. [2010] “Nonlinear stability analysis of the emden-fowler equation,” *J. Nonlin-*
470 *era. Math. Phys.* **17**, 503–516.
- 471 Bröcker, T., & Lander, L. [1975] *Differentiable Germs and Catastrophes*, (Lect. Note Series, 17, London
472 Math. Soc.).
- 473 Cartan, E. [1933] “Observations sur le mémoire précédent,” *Math. Z.* **37**, 619–622.
- 474 Chern, S.S. [1939] “Sur la géométrie d’un système d’équations différentielles du second ordre,” *Bull. Sci.*
475 *Math.* **63**, 206–212.
- 476 Chen, Y. & Yin, Z. [2019] “The Jacobi stability of a Lorenz-type multistable hyperchaotic system with a
477 curve of equilibria,” *Int. J. Bifurcat. Chaos* **29**, 1950062.
- 478 Chen, B., Liu, Y., Wei, Z. & Feng, C. [2020] “New insights into a chaotic system with only a Lyapunov
479 stable equilibrium,” *Math. Methods Appl. Sci.* **43**, 9262–9279.
- 480 Douglas, J. [1927] “The general geometry of paths,” *Ann. Math.* **29**, 143–168.
- 481 Dănilă, B., Harko, T., Mak, M.K., Pantaragphong, P. & Sabău, S.V. [2016] “Jacobi stability analysis of
482 scalar field models with minimal coupling to gravity in a cosmological background,” *Adv. High Ene.*
483 *Phys.* **2016**, p. 26.
- 484 Feng, C., Huang, Q., & Liu, Y. [2020] “Jacobi analysis for an unusual 3D autonomous system,” *Int. J.*
485 *Geom. Methods Mod. Phys.* **17**, 2050062.
- 486 Fujimori, S., Saji, K., Umehara, M., & Yamada, K. [2008] “Singularities of maximal surfaces,” *Math. Z.*
487 **259**, 827.
- 488 Gilmore, R. [1981] *Catastrophe Theory for Scientists and Engineers*, (Dover, New York).
- 489 Gupta, M. K., & Yadav, C. K. [2017] “Jacobi stability analysis of Rössler system,” *Int. J. Bifurcat. Chaos*,
490 **27**, 1750056.
- 491 Gupta, M. K., & Yadav, C. K. [2017] “Jacobi stability analysis of modified Chua circuit system,” *Int. J.*
492 *Geom. Methods Mod. Phys.* **14**, 1750089.
- 493 Gupta, M. K. & Yadav, C. K. [2019] “Rabinovich-Fabrikant system in view point of KCC theory in Finsler
494 geometry,” *J. Interdiscip. Math.* **22**, 219–241.
- 495 Hutchinson G.E. [1948] “Circular causal systems in ecology,” *Ann. NY Acad. Sci.* **50**, 221–246.
- 496 Harko, T. & Sabău, S.V. [2008] “Jacobi stability of the vacuum in the static spherically symmetric brane
497 world models,” *Phys. Rev. D.* **77**, 104009.
- 498 Harko, T., Ho, C.Y., Leung, C.S. & Yip, S. [2015] “Jacobi stability analysis of the Lorenz system,” *Int. J.*
499 *Geo. Meth. Mod. Phy.* **12**, 1550081.
- 500 Harko, T., Pantaragphong, P. & Sabău, S.V. [2016] “Kosambi-Cartan-Chern (KCC) theory for higher-order
501 dynamical systems,” *Int. J. Geo. Meth. Mod. Phy.* **13**, 1650014.
- 502 Hasegawa, M., Honda, A., Naokawa, K., Saji, K., Umehara, M., & Yamada, K. [2015] “Intrinsic properties
503 of surfaces with singularities,” *Internat. J. Math.* **26**, 1540008.
- 504 Huang, Q., Liu, A. & Liu, Y. [2019] “Jacobi stability analysis of the Chen system,” *Int. J. Bifurcat. Chaos*
505 **29**, 1950139.
- 506 Izumiya, S., & Saji, K. [2010] “The mandala of Legendrian dualities for pseudo-spheres in Lorentz-
507 Minkowski space and “flat” spacelike surfaces,” *J. Singul.* **2**, 92–127.
- 508 Izumiya, S., Saji, K., & Takahashi, M. [2010] “Horospherical flat surfaces in hyperbolic 3-space,” *Japanese*
509 *J. Math.* **62**, 789–849.

- 510 Izumiya, S., Romero Fuster, M. D. C., Ruas, M. A. S., & Tari, F. [2016] *Differential Geometry from a*
511 *Singularity Theory Viewpoint*, (World Scientific).
- 512 Klën, W. S. & Molina, C. [2020] “Dynamical analysis of null geodesics in brane-world spacetimes,” *Phys.*
513 *Rev. D* **102**, 104051.
- 514 Kokubu, K., Rossman, W., Saji, K., Umehara U., & Yamada, K. [2005] “Singularities of flat fronts in
515 hyperbolic 3-space,” *Pacific J. Math.* **221**, 303 – 351.
- 516 Kolebaje, O. & Popoola, O. [2019] “Jacobi stability analysis of predator-prey models with holling-type II
517 and III functional responses,” *AIP Conf. Proc.* **2184**, 060001.
- 518 Kosambi D.D. [1933] “Parallelism and path-spaces,” *Math. Z.* **37**, 608–618.
- 519 Krylova, N., Voynova, Y. & Balan, V. [2019] “Application of geometrical methods to study the systems of
520 differential equations for quantum-mechanical problems,” *J. Phys. Conf. Ser.* **1416**, 012021.
- 521 Kumar, M., Mishra, T. N. & Tiwari, B. [2019] “Stability analysis of Navier-Stokes system,” *Int. J. Geom.*
522 *Methods Mod. Phys.* **16**, 1950157.
- 523 Lake, M.J. & Harko, T. [2016] “Dynamical behavior and Jacobi stability analysis of wound strings,” *Eur.*
524 *Phys. J.* **76**, 1–26.
- 525 Liu, A., Chen, B. & Wei, Y. [2020] “Jacobi analysis of a segmented disc dynamo system,” *Int. J. Geom.*
526 *Methods Mod. Phys.* **17**, 2050205.
- 527 Liu, Y., Huang, Q. & Wei, Z. [2021] “Dynamics at infinity and Jacobi stability of trajectories for the
528 Yang-Chen system,” *Discrete. Contin. Dyn. Syst. Ser. B* **26**, 3357-3380.
- 529 Liu, Y., Li, C., & Liu, A. [2021] “Analysis of geometric invariants for three types of bifurcations in 2D
530 differential systems,” *Int. J. Bifurcat. Chaos* **31**, 2150105.
- 531 Ludwig, D., Jones, D. D., & Holling, C. S. [1978] “Qualitative analysis of insect outbreak systems: the
532 spruce budworm and forest,” *J. Anim. Ecol.* **47**, 315–332.
- 533 Martins L.F., & Saji, K. [2016] “Geometric invariants of cuspidal edges,” *Canad. J. Math.* **68**, 445–462.
- 534 Martins, L.F., Saji, K., Umehara M., & Yamada, K. [2016] “Behavior of Gaussian curvature and mean
535 curvature near non-degenerate singular points on wave fronts,” *Geometry and Topology of Manifolds*
536 (Springer, Tokyo), 247–281
- 537 Mishra, T. N., & Tiwari, B. [2021] “Stability and bifurcation analysis of a prey-predator model,” *Int. J.*
538 *Bifurcat. Chaos* **31**, 2150059.
- 539 Mori, A. S. [2011] “Ecosystem management based on natural disturbances: hierarchical context and non-
540 equilibrium paradigm,” *J. Appl. Ecol.* **48**, 280–292.
- 541 Neagu, M. [2013] “Multi-time Kosambi-Cartan-Chern invariants and applications,” *BSG Proceedings.* **20**,
542 36–50.
- 543 Pickett, S. T. [1980] “Non-equilibrium coexistence of plants,” *Bull. Torrey Bot. Club*, **107**, 238–248.
- 544 Porteous, I.R., [2001] *Geometric differentiation. For the intelligence of curves and surfaces* (2nd edition),
545 (Cambridge University Press, Cambridge).
- 546 Poston, T., & Stewart, I. [1978] *Catastrophe Theory and its Applications* (Pitman Publishing Limited,
547 London).
- 548 Raup, D., & Stanley, S. M. [1978] *Principles of Paleontology*, (W.H. Freeman, San Francisco).
- 549 Sabău, S.V. [2005a] “Some remarks on Jacobi stability,” *Nonlinear Anal. TMA.* **63**, e143–e153.
- 550 Sabău, S.V. [2005b] “Systems biology and deviation curvature tensor,” *Nonlinear Anal. RWA.* **6**, 563–587.
- 551 Saji, K., Umehara M., & Yamada, K., [2009] “The geometry of fronts,” *Ann. of Math.* **169**, 491 – -529.
- 552 Saji, K., Umehara M., & Yamada, K., [2010] “The duality between singular points and inflection points
553 on wave fronts,” *Osaka J. Math.* **47** 591–607.
- 554 Saji, K., & Teramoto, K. [2020] “Dualities of differential geometric invariants on cuspidal edges on flat
555 fronts in the hyperbolic space and the de Sitter space,” *Mediterr. J. Math.* **17**, 1–20.
- 556 Salnikova, T. V., Kugushev, E. I. & Stepanov, S. Y. [2020] “Jacobi stability of a many-body system with
557 modified potential,” *Doklady Mathematics* **101**, 154–157.
- 558 Scheffer, M., Bascompte, J., Brock, W. A., Brovkin, V., Carpenter, S. R., Dakos, V., Held H., Van Nes,
559 E.H., Rietkerk, M., & Sugihara, G. [2009] “Early-warning signals for critical transitions,” *Nature* **461**,
560 53.
- 561 Shiba, S., & Umehara, M. [2012] “The behavior of curvature functions at cusps and inflection points,”

- 562 *Differential Geom. Appl.* **30**, 285–299.
- 563 Strogatz, S.H. [2014] *Nonlinear Dynamics and Chaos: with Applications to Physics, Biology, Chemistry,*
564 *and Engineering*, (Westview press, USA).
- 565 Sprugel, D. G. [1991] “Disturbance, equilibrium, and environmental variability: what is ‘natural’ vegetation
566 in a changing environment?,” *Biol. Conserv.* **58**, 1–18.
- 567 Sulimov, V. D., Shkapov, P. M. & Sulimov, A. V. [2018] “Jacobi stability and updating parameters of
568 dynamical systems using hybrid algorithms,” *IOP Conf. Ser. Mater. Sci. Eng.* **468**, 012040.
- 569 Thom, R. [1972] *Stabilité Structurelle et Morphogénèse*, (Benjamin, New York).
- 570 Thompson, J.M.T. [1982] *Instabilities and Catastrophes in Science and Engineering* (John Willy & Sons,
571 New York).
- 572 Udriște, C. & Nicola, I.R. [2009] “Jacobi stability of linearized geometric dynamics,” *J. Dyn. Syst. Geom.*
573 *Theor.* **7**, 161–173.
- 574 Umehara, M. [2011] “A simplification of the proof of Bol’s conjecture on sextactic points,” *P. JPN Acad.*
575 *A-Math.* **87**, 10–12.
- 576 Wang, F., Liu, T., Kuznetsov, N. V., & Wei, Z. [2021] “Jacobi stability analysis and the onset of chaos in
577 a two-degree-of-freedom Mechanical System,” *Int. J. Bifurcat. Chaos* **31**, 2150075.
- 578 Wright, E. M. [1955] “A non-linear difference-differential equation,” *J. Reine Angew. Math.* **194**, 66–87.
- 579 Yajima, T., Yamasaki, K., & Nagahama, H. [2018] “Non-holonomic geometric structures of rigid body
580 system in Riemann-Cartan space,” *J. Phys. Commun.* **2**, 085008.
- 581 Yamasaki, K. & Yajima, T. [2013] “Lotka-Volterra system and KCC theory: Differential geometric structure
582 of competitions and predations,” *Nonlinear Anal. RWA.* **14**, 1845–1853.
- 583 Yamasaki, K. & Yajima, T. [2016] “Differential geometric structure of non-equilibrium dynamics in com-
584 petition and predation: Finsler geometry and KCC theory,” *J. Dyn. Syst. Geom. Theor.* **14**, 137–153.
- 585 Yamasaki, K. & Yajima, T. [2017] “KCC analysis of the normal form of typical bifurcations in one-
586 dimensional dynamical systems: Geometrical invariants of saddle-node, transcritical, and pitchfork
587 bifurcations,” *Int. J. Bifurcat. Chaos*, **27**, 1750145.
- 588 Yamasaki, K. & Yajima, T. [2020] “KCC Analysis of a one-dimensional system during catastrophic shift of
589 the Hill function: Douglas tensor in the nonequilibrium region,” *Int. J. Bifurcat. Chaos*, **30**, 2030032.
- 590 Zeeman, E.C. [1977], *Catastrophe Theory: Selected Papers 1972-1977* (Addison-Wesley, Boston).